



Journal Name

ARTICLE

Nanocontainer-based self-healing coatings: current progress and future perspectives

Elena Shchukina,^a Hongqiang Wang^b and Dmitry G. Shchukin,^{*a}

Received 00th January 20xx,
Accepted 00th January 20xx

DOI: 10.1039/x0xx00000x

www.rsc.org/

Here, we summarize the recent achievements in the field of the nanocontainer-based self-healing coatings done during the last 8 years. The development of the nanocontainer-based self-healing coatings has been started 15 years ago from the study of the nanocontainers with stimuli responsive release properties able to release anticorrosion agent (inhibitor) on demand only into corroded area thus preventing its spontaneous leakage. Since that, many different types of the nanocontainers have been demonstrated: from polymer capsules to the porous inorganic nanoparticles with sophisticated mechanism of the release triggering. Nowadays, the study of the commercial application of the nanocontainer-based self-healing coatings is the main focus in this area, especially for the coatings with several autonomic functionalities. However, the search for the new types of the multifunctional nanocontainers possessing different triggering mechanisms is still remained active, especially for low-cost natural nanocontainers.

The more and more new automated systems influence on the economy and human life during the last 50 years. Most of them, of course, are related to the very rapid progress in computing technologies which changes the information environment of the humans. Unfortunately, the development of the smart materials with self-responding properties on micro and nanoscale has been started much later in 80th. Here, we would like to highlight one of the universal approaches for fabrication of the autonomous materials based on the encapsulation of the active agents into micro and nanosized containers (capsules) with the controlled release properties of the shell. This approach can be applied to the different types of smart materials with multiple responsive functionalities. However, due to the main expertise of the authors and limited journal space, we focus this highlights minireview on nanocontainer-based self-healing coatings.

The concept of such type of the coatings combines the classic passive component of the coating –matrix (layer) and active component – nanocontainers loaded with corrosion inhibitors or other active agents which possess controlled permeability of the shell (Figure 1).^{1,2} This allows one to joint in one coating classical passive functionalities like barrier, colour together with active ones responsive to the both internal and external impacts like cracks, local pH, electrochemical potential, temperature, humidity, etc.

The main difficulty in “nanocontainer” approach is to develop nanocontainer shell with controlled permeability specific to several triggers and, at the same time, stable inside the coating formulation as well as during coating application and curing. Another challenge is the uniform distribution of the nanocontainers in the coating. Formation of the any aggregates will (i) damage the coating integrity in the aggregated area and (ii) leave some parts of the coatings without self-healing ability.

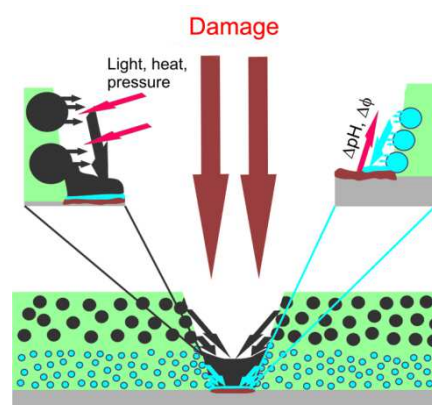


Fig. 1 Concept of the nanocontainer-based self-healing coatings.²

Mechanical impact was the first external stimulus demonstrated for capsule-based self-healing coatings by the group of S. R. White in 2001.³ They encapsulated healing agent (dicyclopentadiene) into polymer microcapsules embedded in an epoxy matrix containing Grubbs catalyst. Embedded microcapsules were ruptured inside the coating crack releasing healing agent, which entered into the contact with the embedded catalyst. The resulting polymerization of the healing agent leads to the crack healing and recovery of the barrier properties of the coating. Simultaneous incorporation of two types of capsules containing different active agents⁴ or capsules filled with reactive epoxy resin or oil^{5,6} was also reported. Encapsulation of moisture or oxygen reactive materials, such as metal oxide precursors⁷, or linseed oil⁸ adapts nanocontainer response to atmospheric oxygen or humidity forming impermeable layer in the damaged part of the coating.

pH shift occurring on the metal substrate surface during the corrosion process is the second, and now most popular, trigger studied for self-healing coatings for corrosion protection. The corrosion process is associated with local pH decrease in anodic area and local pH increase in cathodic one. Therefore, the nanocontainer shell sensitive to either both or one of acidic and alkaline regions can

^a Stephenson Institute for Renewable Energy, Department of Chemistry, University of Liverpool, L69 7ZF Liverpool, UK. Corresponding author Prof. Dmitry Shchukin, d.shchukin@liverpool.ac.uk.

^b Centre for Nanoenergy Materials, School of Materials Science and Engineering, Northwestern Polytechnical University, Xi'an, 710072, P. R. China.

release encapsulated inhibitor for corrosion termination. Polyelectrolyte capsules,⁹ polymeric micro/nano-sized capsules formed by interfacial polymerization,¹⁰ hydrogels¹¹ and porous nanoparticles with bioinspired nanovalves^{12–14} having weak acidic or basic functional groups in the shell were presented in the literature for reversible and (or) irreversible changes of the shell permeability in a wide pH range (e.g., at low pH < 4 or high pH > 9).

More rare external triggers used for capsules and nanocontainers in self-healing coatings are: (1) electromagnetic irradiation, the container shell should have sensitive components like metal (silver) nanoparticles for IR light,^{15,16} dyes for visible light¹⁷ and semiconductors (TiO₂ nanoparticles) for UV light;¹⁸ (2) ultrasonic treatment;¹⁹ (3) temperature;²⁰ (4) ionic strength;²¹ (5) electrochemical potential on the surface of the corroded metal substrate.^{22, 23, 24}

The current level of the development of nanocontainers for self-healing coatings with single functionality or responsive only to one triggering mechanism already achieved sufficient number of demonstrations on the laboratory scale and requires now the steps for industrial implementations using low cost, effective nanocontainers. The presented Highlight paper is the follow-up of our first highlights paper in the area of nanocontainers and self-healing coatings published in 2011.²⁵ The main aim of this minireview is to discuss the current trends in the second generation of the self-healing coatings possessing multifunctionality, active to multiple triggering mechanisms and low-cost nanocontainers for application in industry.

Nanocontainers for industrial application in self-healing coatings

All nanocontainers (capsules) can be divided into two classes by their nature: polymer nanocontainers (core-shell capsules, gels) and inorganic nanocontainers (porous inorganic materials). Polymer nanocontainers require multi-step technology for their fabrication including polymerisation reactions, encapsulation of inhibitor, washing, removal and utilization of the reaction by-products and non-reacted reagents. Their fabrication also requires quite sophisticated equipment. On the contrary, commercially available porous inorganic materials can be applied as inorganic nanocontainers for self-healing coatings. Only inhibitor loading and formation of the trigger-sensitive blockers (valves) are fabrication steps required to produce ready-to-use inhibitor-loaded nanocontainers. Inorganic nanocontainers could be mesoporous silica²⁶ or titania,²⁷ ion-exchange nanoclays²⁸ and halloysite nanotubes.²⁹ Mesoporous silica and titania are commercial products and, despite they are produced in thousand tons volume, they are still more expensive than raw materials: ion-exchange clays and halloysites. The last two types of nanocontainers can be mined from different deposits and used after purification for inhibitor loading and further as self-healing additive in coatings.

Ion-exchange nanoclays as nanocontainers

There are two types of ion-exchange release of the entrapped inhibitor from nanoclays: the less studied cation-exchange release and the more developed anion-exchange release.³⁰ Both of them have similar mechanism of the uptake and release of the corrosion inhibitors loaded between the layers (Figure 2). The only difference is in the triggers initiating the release.

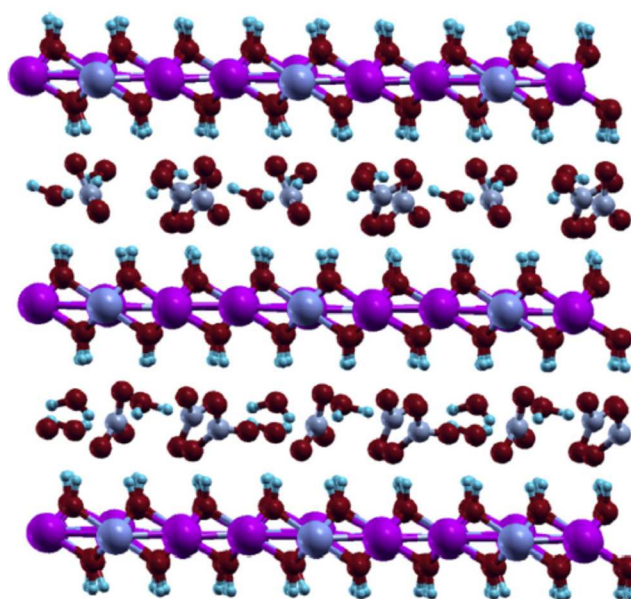


Fig. 2 Schematic presentation of the layered nanoclay structure.³¹ Inhibitor molecules (small) are uploaded within interlayer galleries between nanoclay layers.

If the nanoclay layers are charged negatively, only positively charged inhibitor can be uploaded in the interlayer galleries to compensate the negative charge. The same mechanism is for the positively charged nanoclay layers – only negatively charged corrosion inhibitor can be uploaded. The release for nanoclay-based nanocontainers is triggered by ion-exchange in the presence of H⁺, OH⁻, Cl⁻ and other corrosion products or aggressive ions.³¹

However, the release of the inhibitor in cation-exchanger clays can only be triggered by metal cations available in the surrounding environment, which may not be directly associated with corrosion processes leading to the uncontrolled release of the inhibitor. Bentonite is a cation-exchanger and one of the rare examples of nanocontainers for self-healing coatings, consisting of stacks of negatively charged aluminosilicate sheets between which inhibiting cations like Ca²⁺ and Ce³⁺ were intercalated.^{32,33} Ce-loaded bentonites dispersed in polyester resin layers and applied to galvanized steel substrates display active protection avoiding coating decomposition. Ce-loaded bentonites were also combined with Ce-exchanged Shieldex[®] and dispersed in polyvinyl butyral coatings applied to hot dip galvanized steel showing the decrease of the coating delamination. The protective performance of Na-montmorillonite (Na-MMT) intercalated with zinc cations (Zn-MMT), benzoimidazole (BIAMMT) and the mixture of these two inhibitors (Zn-MMT + BIAMMT) is described as an example of another cation-exchanging natural clay material for self-healing anticorrosion coatings.³⁴ The modified clay particles were added to the epoxy ester coating. The interlayer distance of the clay particles was increased after Na⁺ cations exchange with inhibitors. The highest corrosion resistance and the lowest adhesion loss were observed when the mixture of Zn-MMT and BIAMMT clay nanocontainers was used. The crack filling behaviour of the transparent, multilayer coating consisting of a polysiloxane film on top of a thin montmorillonite interlayer was monitored using confocal and SEM microscopy.³⁵ Filling of cracks in the polymeric topcoat occurred primarily within the first two hours of exposure to the moisture saturated air and resulted in a restoration of the surface flatness. Beyond the 2 h

healing period, further expansion of the clay layers resulted in restoration of the barrier properties of the coating.

The anion-exchanging clays are more effective in controlling the behavior of corrosion inhibitor in the coating than the cation-exchanging ones. For anion-exchange clays, not only release of the corrosion inhibitors but also trapping of the corrosive agents (Cl^- , SO_4^{2-}) are efficient for autonomic corrosion protection. Layered double hydroxides (LDHs) have general formula $[\text{M}^{2+}_{1-x}\text{M}^{3+}_x(\text{OH})_2]\text{A}^{n-}_{x/n}\cdot m\text{H}_2\text{O}$, where the cations M^{2+} (Mg^{2+} , Zn^{2+} , Fe^{2+} , Co^{2+} , Cu^{2+} and others) and M^{3+} (Al^{3+} , Cr^{3+} , Fe^{3+} , Ga^{3+} and others) occupy the octahedral holes in a brucite-like layer and the anion A^{n-} is located in the hydrated interlayer galleries.³⁶ As an example of LDH, Figure 3 represents the plate structure of $\text{Zn-Al-NO}_3\text{-LDH}$.³⁷

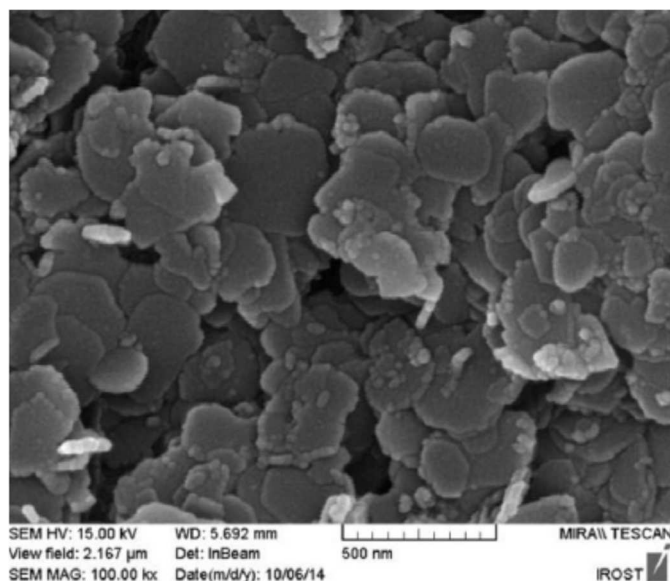


Fig. 3 SEM image of $\text{Zn-Al-NO}_3\text{-LDH}$.³⁸

The thickness of the LDH plates is usually about 30–50 nm. Williams *et al.* prepared LDHs with different organic inhibitors (benzotriazole, ethyl xantate and oxalate).³⁸ The resulting inhibitor-loaded LDHs were inserted into a poly(vinylbutyral) coating on the top of AA2024-T3 aluminium alloy. In another report, Kendig and Hon prepared LDHs intercalated with 2,5-dimercapto-1,3,4-thiadiazolate and studied the inhibiting properties of this anion with respect to the oxygen reduction reaction on copper.³⁹ Zn-Al and Mg-Al LDHs loaded with quinaldate and 2-mercaptobenzothiazolate were synthesized *via* anion-exchange reaction.⁴⁰ Spectrophotometric measurements confirmed the release of organic anions from LDHs into the bulk solution triggered by chloride anions. The coating barrier properties were found to be the best for LDH-doped primer. Poznyak *et al.*⁴¹ showed active corrosion protection of aluminium alloy 2024-T3 for coatings with LDHs intercalated with 2-mercaptobenzothiazole and quinaldic acid.

An additional improvement of the self-healing activity can be achieved by using simultaneously inhibitor-loaded LDHs and cerium molybdate nanocontainers loaded with mercaptobenzothiazole added into epoxy primers, either individually or in 1:1 combination.⁴² The evolution of the self-healing activity was studied by the scanning vibrating electrode technique (SVET) with a defect (0.2 mm size) created in the coating prior to immersion into 0.05 M NaCl solution (Figure 4).

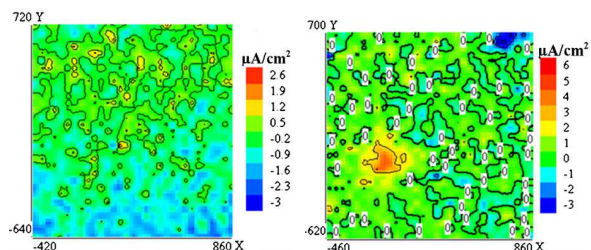


Fig. 4 Coating modified with a mixture of mercaptobenzothiazole-LDH and cerium molybdate nanocontainers. Current density maps obtained at immersion times in 0.05 M NaCl: after 3 h (left) and after 40 h (right).⁴²

The coating without nanocontainers revealed the corrosion immediately after immersion in 0.05 M NaCl and the corrosion anodic current increased continuously with time. The coating with mercaptobenzothiazole-loaded LDH demonstrated only almost negligible corrosion activity after 40 h of immersion (Figure 4). The addition of a mixture of nanocontainers results in a synergetic inhibition effect that combines early corrosion protection and longer term inhibition. Such behaviour clearly demonstrates the potential of nanocontainer mixtures in the design of smart coatings with self-healing abilities for prolonged coating lifetime. Similar synergetic effect was reported for only LDH nanocontainers but loaded with different inhibitors: vanadate, phosphate and 2-mercaptobenzothiazole.⁴³ The combination of LDH nanocontainers loaded with vanadate and phosphate anions, and vanadate and mercaptobenzothiazole (MBT) anions conferred a significant improvement in corrosion protection on AA2024 aluminium alloy. Hydrotalcite-based conversion films also demonstrated perfect corrosion protection.⁴⁴ The hydrotalcites are typical anion-exchange materials consisting of stacks of positively charged mixed hydroxide layers separated by anions and water molecules. An environmentally friendly corrosion inhibitor, phytic acid, was successfully added to the hydrotalcite film by adsorption and ion-exchange.⁴⁵ The metal substrate used in this study was AZ31 Mg alloy. Compared with the original hydrotalcite film, the corrosion behaviour of the hydrotalcite film with intercalated phytic acid is much better. The resistance was notably higher than that of the original hydrotalcite film after 12 h immersion. The same group demonstrated the performance of molybdate intercalated into hydrotalcite particles for magnesium protection.⁴⁶ By means of competitive adsorption, protective deposition and oxidation reactions, the released MoO_4^{2-} ions acted as a good anodic inhibitor to protect Mg alloys from corrosion attacks.

The price for the ion-exchange nanoclays as nanocontainer host varies between 90 – 3600 USD per metric ton depending on the nature of the nanoclays. The abundant of the supply sources together with the low cost is the main advantage of the ion-exchange nanoclays to be applied for industrial self-healing coatings. However, the main disadvantage is their low loading inhibitor capacity. Layered mineral clays can only load corrosion inhibitor between their layers in a small, 0.5–2 nm sized lumen. This results in a low loading capacity of the clays, which is usually 5–8 wt%. One needs to find possibility to increase the loading capacity of nanocontainers in order to prolong service lifetime of self-healing materials. The more corrosion inhibitor loaded into the containers, the larger the corrosion defect that can be healed.

Halloysite nanocontainers

Halloysite is a clay material that can be mined from deposits as a raw mineral (price range 6-10 USD per kg).^{47,48} Halloysite ($\text{Al}_2\text{Si}_2\text{O}_5(\text{OH})_4 \cdot n\text{H}_2\text{O}$) is a layered aluminosilicate chemically similar to kaolin which has a hollow tubular structure in the submicrometer range. The size of halloysite tubules varies from 500-1000 nm in length and 15-100 nm in inner diameter depending on the deposit (Figure 5).

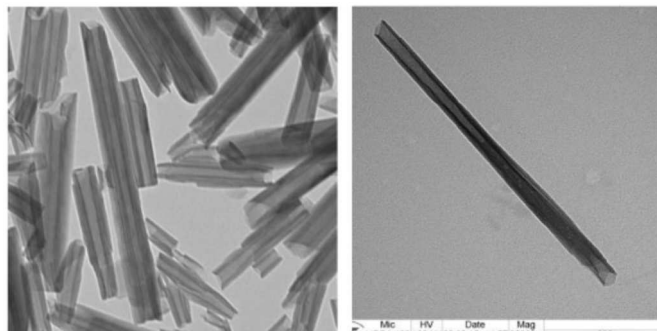


Fig. 5 TEM images of halloysite nanotubes.⁴⁹

The neighbouring alumina and silica layers together with their hydrated water, create a packing disorder causing them to curve and roll up, forming multilayer tubes. The reason flat kaolinite rolls into halloysite tubules remains unclear.⁴⁹ There are between 15-20 aluminosilicate layers rolled in the multilayer tubule walls with a layer spacing of 0.72 nm for the dehydrated halloysite. The typical specific surface area of halloysite is 65 m^2/g , pore volume is 1.3 mL/g and specific gravity is 2.53 g/cm^3 . The outermost surface of the halloysite is relevant to silica while the inner lumen surface may be compared to alumina. Below pH 8.5 the tubule lumen has a positive inner surface, enabling loading of negative corrosion inhibitor and preventing its adsorption on the negatively charged outer surface. The current world supply of halloysites is in excess of 50 000 tons per year.

Inner halloysite lumen can provide additional space and increased loading capacity for corrosion inhibitors up to 20 wt%.⁵⁰ Additional selective etching of the alumina inside halloysite lumen with sulfuric acid can increase lumen capacity and corrosion inhibitor loading up to 60 wt%.⁵¹ This loading capacity is close to the loading capacity of polymer nanocontainers. Besides corrosion inhibitors, halloysite can be a cargo for biocides and exploited in antifouling coatings.^{52,53} The typical procedure of the loading of halloysite nanotubes is as follows.⁵⁴ Halloysites are mixed with a solvent possessing high solubility for the desired corrosion inhibitor and low temperature boiling point. Then, the vial containing the solution is placed in a desiccator under vacuum, which deaerates the halloysite lumen. Due to the rapid evaporation of the solvent, the inhibitor concentration increases thus improving the loading efficiency.

Embedding of the inhibitor-loaded halloysites into the coating requires intensive mixing of the dried halloysites with the coating formulation using high-speed stirrers, UltraTurrex or ultrasound. Formation of any aggregated nanocontainers will make defects in the coating integrity thus reducing coating barrier properties. The halloysite should be homogeneously distributed on the coated area to protect every part of the metal substrate (Figure 6).

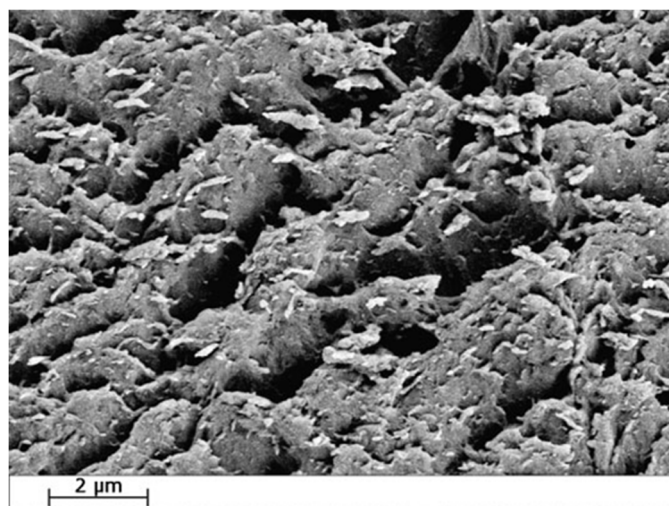


Fig. 6 Distribution of inhibitor-loaded halloysite nanotubes inside a sol-gel coating.⁵⁴

The self-healing properties of benzotriazole and 8-hydroxyquinoline-loaded halloysite nanotubes were studied in zirconia-silica sol-gel coatings deposited on the surface of aluminium alloy A2024 by periodic measurements of SVET current density profiles.⁵⁵ Migration of the corroding centre along the defect appeared for aluminium plates coated with pure sol-gel film. This is not the case for hybrid films containing halloysite nanocontainers. SVET observations on aluminium plates coated with sol-gel films containing inhibitor-loaded halloysite revealed the reduction of maximal anodic current down to the noise level within 4.5 hours of immersion in 0.1 M NaCl. Halloysite clay nanotubes loaded with corrosion inhibitors benzotriazole, mercaptobenzimidazole and mercaptobenzothiazole were used as additives in self-healing composite paint coating of copper.^{56,57} The release rate of benzotriazole was controlled by the formation of metal-benzotriazole stoppers at tube endings. This method provided high halloysite loading efficiency and a long release time which gives additional possibilities for process optimization. Formation of the insoluble metal-benzotriazole complex was studied for Cu(II), Fe(II), Fe(III) and Co(II) ions. The best release control was achieved for the Cu-benzotriazole complex. Corrosion tests were performed on 110 copper alloy strips. A green patina observed underneath the bare paint for the blank sample indicates severe corrosion. Halloysites loaded with corrosion inhibitors significantly reduced corrosion in all the composite coatings. Small corrosion activity was observed within the first 15 days but then it was suppressed with the release of inhibitors in the coating defects. The efficiency of the halloysite lumen loading ascended in the order of benzotriazole < mercaptobenzothiazole < mercaptobenzimidazole. Recently, another type of the ceramic nanotubes called attapulgite was introduced as an alternative for halloysite nanocontainers.⁵⁸ Attapulgite (ATP) is a hydrous layer-ribbon magnesium aluminum silicate with a fibrous structure and a theoretical formula of $(\text{Al}_2\text{Mg}_2)\text{Si}_8\text{O}_{20}(\text{OH})_2(\text{OH}_2)_4 \cdot 4\text{H}_2\text{O}$.⁵⁹ The ATP nanoparticles possess a fibre-shaped morphology with a size of approximately 0.8–1 μm long and 20 nm in diameter. ATP is widely used as a reinforcement filler of nanocomposites, catalyst carrier, and adsorbent. ATP was found to be a viable and inexpensive nanoscale container and in industry, the price of ATP is about 200 USD per ton.⁶⁰ A composite ATP/PEI/PSS/BTA/PSS/BTA nanocontainers incorporated into a water-based epoxy demonstrated advanced self-healing properties and maximum BTA release achieved at pH 10.

Despite the large number of papers devoted to nanocontainer-based self-healing coatings, most of them use lab-scale analytical methods for characterization of their self-healing performance. The current level of the development of nanocontainer-based self-healing coatings appeals for the study of the perspectives for industrial applications. Anticorrosion performance tests using the industrial neutral salt-spray test (ISO 9227 standard, 5 wt% NaCl, 35 °C) were conducted to check halloysite efficiency in industrial coatings.^{61,62}

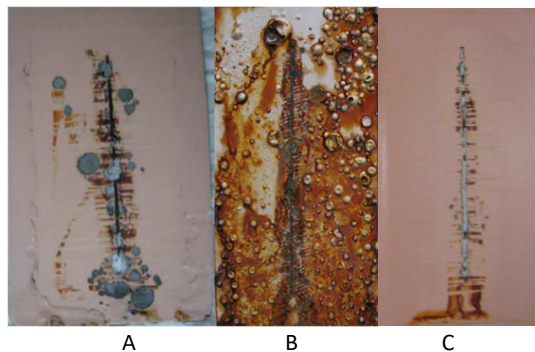


Fig. 7 Neutral salt-spray test results for pure polyepoxy coating (A, 1000 h), polyepoxy coating directly loaded with Korantin SMK corrosion inhibitor (B, 500 h) and polyepoxy coating in the presence of Korantin SMK-loaded halloysite nanotubes (C, 1000 h).⁶¹

Standard commercial polyepoxy coating was used for comparison. As one can see in Figure 7, direct addition of Korantin SMK corrosion inhibitor, which is an alkylphosphoric ester produced by BASF with a chain length of alkyls in the ester group ranging from C6 to C10, into the coating in free form (1 wt%) drastically reduces corrosion protection performance after 500 h of the neutral salt-spray test. On the contrary, inhibitor encapsulated inside halloysite nanotubes increased corrosion protection by five times. This is clear evidence on the industrial level, employing a widely known salt-spray industrial tests, that halloysite nanotubes can develop a new, revolutionary generation of self-healing anticorrosion coatings.

Multifunctional nanocontainers

The multiple functionality of the coatings is limited by the amount of nanocontainers (capsules) which can be incorporated into the coatings without changing their main properties like barrier, colour, etc. Usually, if the amount of nanocontainers exceeds 10 wt% in the cured coating, its main passive functionalities become considerably reduced.⁶³ Therefore, the second generation of the multifunctional nanocontainer based coatings should not have a combination of the nanocontainers with single functionality, but involve nanocontainers with multiple functionalities. This direction is rapidly developing now with the increasing number of publications.

Multifunctional nanocontainers can be divided into two types. First type has the shell sensitive to the several (two or more) triggers. The second one can contain either cargo with several functionalities or combination of primary functionality of the cargo with the secondary functionality of the shell.

One of the mostly developed combinations is the use of several corrosion inhibitors in one nanocontainer. The combination of the corrosion inhibitors active at different conditions (e.g., pH, temperature) can provide synergistic effect for self-healing efficiency of the coatings. Composite cerium molybdate nanocontainers were synthesized and then loaded with 8-hydroxyquinoline or with 1-H-benzotriazole-4-sulfonic acid.⁶⁴ First, polystyrene nanospheres were

produced using emulsion polymerization. Then, the polystyrene spheres were coated to form a cerium molybdate layer via the sol-gel method followed by calcination. The resulting cerium molybdate capsules were loaded with the organic inhibitor. Application of cerium molybdate nanocontainers loaded with mercaptobenzothiazole (58 wt%) was also shown for the protection of magnesium alloys.⁶⁵ Spontaneous emulsification method was exploited to prepare mesoporous CeO₂@SiO₂ hybrid particles for the corrosion protection of aluminium.⁶⁶ To complement CeO₂ corrosion inhibition, 8-hydroxyquinoline was used, which is an effective anodic inhibitor that exhibited synergistic effects with Ce-containing compounds. These two encapsulated inhibitors provided effective corrosion protection of aluminium by two mechanisms: the initial burst of encapsulated 8-hydroxyquinoline following by the sustained release of the Ce ions. Hollow CeO₂ nanocontainers were prepared as reservoirs for loading benzotriazole (BTA) inhibitor. Then, the loaded CeO₂ nanocontainers were coated with polyelectrolyte multilayers by layer-by-layer deposition approach to form a core-shell structure of CeO₂/BTA/(polyethylene imine, PEI/polystyrene sulphate, PSS)₂.⁶⁷ The modified CeO₂ nanocontainers were incorporated into the epoxy coating at a concentration of 0.5 wt%. The size of the CeO₂ particles is around 200–230 nm in diameter. The release curve at pH 7 demonstrates control of the PEI/PSS polyelectrolyte shell over BTA spontaneous release avoiding undesirable leakage due to its weak permeability properties in the neutral aqueous condition. When the pH values change to acidic or alkaline conditions, the BTA molecules release from the nanocontainers much faster (Figure 8). This is attributed to the polyelectrolyte shells with weak acidic or basic ionisable functional groups. These groups can demonstrate reversible and/or irreversible changes of the shells permeability in a wide pH region (e.g. at low pH < 4 and high pH > 9).⁶⁸ The Scanning Kelvin Probes maps of Volta potential distribution after immersion in 0.5 M NaCl demonstrated no corrosion effects around the defect of the coating containing double-inhibiting nanocontainers.

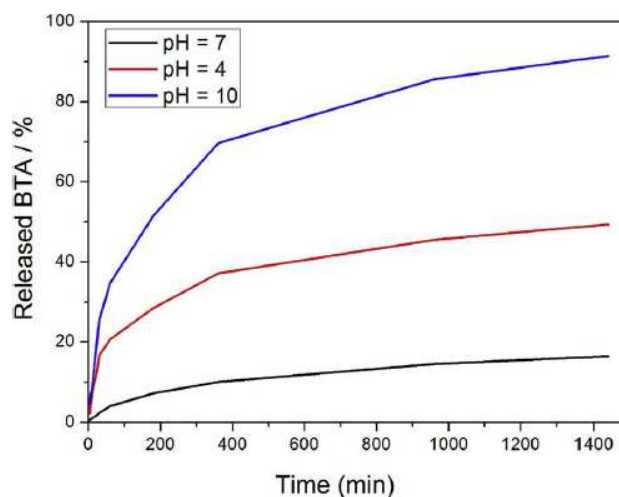


Fig. 8 BTA release profiles from CeO₂/BTA/(PEI/PSS)₂ nanocontainers.⁶⁷

Multishelled capsules containing linseed oil as a main core inhibitor and benzotriazole between polyelectrolyte multilayers were prepared by combination of *in-situ* polymerisation and polyelectrolyte layer-by-layer assembly technique.⁶⁹ FTIR analyses and zeta potential measurements confirmed the encapsulation of

the linseed oil inside and the effective adsorption of alternate layers of polyethylene imine, polystyrene sulphonate and benzotriazole in the shell. The electrochemical impedance spectroscopy analysis of the coated AISI 1020 carbon steel showed pronounced self-healing effect of the epoxy resin loaded with 4.8 wt% of double stimuli-responsive capsules.

Novel benzotriazole loaded nanocontainers with additional shell functionality were developed using tannic acid-Fe (III) complex (TAC) as the shell and benzotriazole as a loaded inhibitor.⁷⁰ The deposition of TAC as a shell for BTA-loaded nanocontainers takes only 20 s. The Electrochemical Impedance of blank coating presented the downward trend during 20 days. In terms of coatings with nanocontainers-BTA@TAC, the impedance modulus at 0.01 Hz increased from $4.7 \times 10^4 \Omega \text{ cm}^2$ to $1.8 \times 10^5 \Omega \text{ cm}^2$. Both the released BTA and the detached tannic acid from the surface of mesoporous silica nanoparticles are contributed to the self-healing effect of the coatings.

Triple-action self-healing polymer coatings were developed by incorporation of dual-function capsules containing polycaprolactone (PCL) and the corrosion inhibitor 8-hydroxyquinoline (8HQ) into shape memory polymer coating (SMP).⁷¹ The results demonstrated that the coating possessed a triple-action self-healing ability enabled by the cooperation of the 8HQ inhibitor, the SMP coating matrix, and the melted microspheres. The coating released 8HQ (inhibitor loading is 21 wt%) in a pH-dependent fashion and immediately suppressed corrosion within the coating scratch. After heat treatment, the scratched coating exhibited excellent recovery of its anticorrosion performance attributed to the simultaneous initiation of scratch closure by the shape memory effect of the coating matrix together with sealing of the scratch by the melted microspheres.

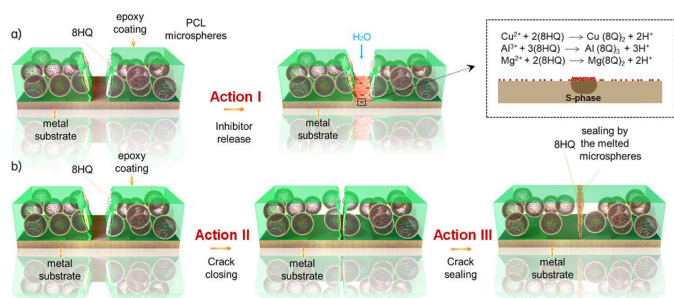


Fig. 9 Triple self-healing mechanism performed by (a) 8HQ released from PCL capsules for local corrosion inhibition, (b) synergetic effect of crack closing by the shape memory epoxy polymer and crack sealing by the melted PCL capsules.⁷¹

As shown in Figure 9, the capsules hold corrosion inhibitor which releases from the capsules and suppressed corrosion when the coating is damaged. When heat was applied, the shape memory effect induced the closure of the coating scratch, which is further sealed by the simultaneous melting of the PCL shell of the capsules. Coatings containing 5, 10, and 15 wt % capsules exhibited a repaired barrier effect after heating at 80 °C for 30 min. The full recovery of barrier properties of the coating was attributed to not only the closure of the scratch by the shape memory effect but also the sealing of the remaining gaps by the melted PCL capsules. An optimum quantity of 10 wt % microspheres was defined by assessing the morphology and barrier properties of the coatings. The presence of corrosion inhibitor 8HQ is necessary to passivate underneath

surface of the Al substrate before crack closure with polymer components of the coating in order to prevent further interaction with corrosive species, which can diffuse through the healed/initial interface of the coating.

The multifunctional encapsulation in nanocontainers can be challenging when the organic chemical species to be encapsulated have different polarities.⁷² A new design for nanocontainers that allows for a selective release of one encapsulated agent by pH change and another agent by chemical reduction of the nanocontainer shell is demonstrated by Crespy *et al.*⁷³ Polyaniline (PANI) was selected as material to build the shell of the nanocontainers. The PANI structure has the important advantage to be both redox and pH responsive. The two selected corrosion inhibitors were 3-nitrosalicylic acid (3-NisA) and 2-mercaptobenzothiazole (MBT). The first molecule has a pKa value around 3 and therefore its solubility can be controlled by pH while the second molecule can be attached to the covering gold surface and then later released electrochemically. The strategy for the multifunctional release of the two inhibitors is represented in Figure 10.

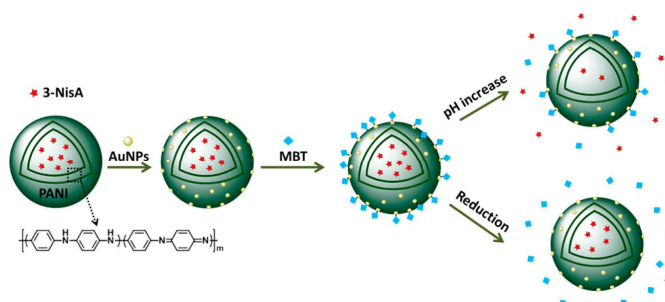


Fig. 10 Scheme representing the formation of the dual-delivery nanocontainers and the subsequent selective release of the corrosion inhibitors upon pH change or reduction.⁷³

The PANI/3-NisA nanocontainers were then successfully decorated with gold nanoparticles (AuNPs, ~20 nm diameter) by electrostatic adsorption. The presence of gold nanoparticles on the PANI shell allows for a stable electronic contact between the capsules and a metal substrate and, at the same time, the presence of the gold nanoparticles on the shell provides a possibility for loading of the MBT via gold-thiol bond. Two encapsulated inhibitors can be released selectively and independently by activating the nanocontainers either by pH change or by electrochemical reduction. Similar approach was explored for designing nanocontainers allowing for the release of two corrosion inhibitors with different release mechanisms.⁷⁴ The first corrosion inhibitor, MBT, was covalently bound to the shell of the nanocontainers. The second one, polydimethylsiloxane diglycidyl ether as hydrophobic healing agent, was physically entrapped in the core of the nanocontainers. The nanocontainers were formed by phase separation in nanodroplets between the polymer and the liquid core induced by the evaporation of low boiling solvent initially present in the nanodroplets. The release of the two self-healing agents was triggered by reduction of the polymeric shell and the release rate actually depended on the

chemical nature of the hydrophobic healing agent and the chemical structure of the shell. Additionally, the release of the MBT from the nanocontainer shell allows for the release of the entrapped hydrophobic self-healing agent yielding a cascade release of the two inhibitors.

Conclusions

The concept of the nanocontainer-based self-healing coatings gained increasing interest among researchers since our first Highlight paper published in 2011 (Chem. Comm., 2011, 47, 8730–8739). The number of publications in this area increased from 80 in 2011 to >300 in 2017 according to the WoS database (“self-healing coatings” have been selected as a topic for literature search). The main advantage of such self-healing coatings is their autonomic response to the corrosion or any other defects in the coating. After the damage is healed, the release for the encapsulated active agents stops and coating restores its characteristics.

This approach has been demonstrated by numerous publications with coatings containing nanocontainers with single function like release of one corrosion inhibitor using one triggering mechanism. There is a great challenge to extend this approach to the development multifunctional nanocontainers able to encapsulate several active materials and respond to different triggering impacts. This can attain the coating autonomic multifunctionality reacting to the various environmental changes. A lot of the research work has to be done in this area, mostly focusing on the mechanisms of coating matrix-shell and nanocontainer-nanocontainer interactions. This will require more efforts in development of new shell components and decrease of the nanocontainer size maintaining, at the same time, high loading capacity.

Another challenge is the transformation of the current research achievements to the technology level. It is more than 15 years of research in this area and now the time is critical to transfer lab results to the practical applications. This work requires close collaboration with paint producers to adapt developed nanocontainers to the commercial paint formulations and industrial tests. Unfortunately, 80 % of the lab results cannot find real industrial application mostly because of the high costs, complexity and low stability of the studied nanocontainers in paint formulations. High ratio between container size and coating thickness can result in the loss of physical integrity of the coating matrix. The nanocontainer shell has to provide good adhesion between containers and host matrix as well as many other properties which are mostly omitted during laboratory research. However, several lab-industry collaborations already exist in UK, USA, EU, China and Russia resulting in few prototypes and even nanocontainer-based self-healing coatings on the market.

The nanocontainer technologies developed for self-healing coatings can be used for other smart materials. A lot of research work remains for detailed mechanism of the controlled shell opening/closing and loading capacity.

Conflicts of interest

There are no conflicts to declare.

Acknowledgements

The work was supported by ERC Consolidator grant ENERCAPSULE (project 647969) and ERC Proof-of-Concept grant ENERPAIN (project 767173). This article is dedicated to the memory of Professor Helmuth Möhwald, one of the co-founders of the Max Planck Institute of Colloids and Interfaces and the only leader of the Department of Interfaces in MPI-KGF.

Notes and references

- 1 D.G. Shchukin and H. Möhwald, *Science*, 2003, **341**, 1458.
- 2 D.G. Shchukin and H. Möhwald, *SMALL*, 2007, **3**, 926.
- 3 S.R. White, N.R. Sottos, P.H. Geubelle, J.S. Moore, M.R. Kessler, S.R. Sriram, E.N. Brown and S. Viswanathan, *Nature*, 2001, **409**, 794.
- 4 M.W. Keller, S.R. White and N.R. Sottos, *Advanced Functional Materials*, 2007, **17**, 2399.
- 5 M.M. Caruso, B.J. Blaiszik, S.R. White, N.R. Sottos and J.S. Moore, *Advanced Functional Materials*, 2008, **18**, 1898.
- 6 X. He and X. Shi, *Progress in Organic Coatings*, 2009, **65**, 37.
- 7 H. Liu, E. Gnade and K.J. Balkus, *Smart Coatings III. ACS Symposium Series*, Chapter 3, 2010, 31.
- 8 C. Suryanarayana, K.C. Rao and D. Kumar, *Progress in Organic Coatings*, 2008, **63**, 72.
- 9 D.G. Shchukin, G.B. Sukhorukov, *Adv. Mater.*, 2004, **16**, 671.
- 10 A. Latnikova, D.O. Grigoriev, J. Hartmann, H. Mohwald and D.G. Shchukin, *Soft Matter*, 2011, **7**, 369.
- 11 A. Latnikova, D.O. Grigoriev, H. Mohwald and D.G. Shchukin, *Polymer*, 2015, **73**, 183.
- 12 M.M. Boyle, R.A. Smaldone, A. C. Whalley, M.W. Ambrogio, Y.Y. Botros and J.F. Stoddart, *Chem. Sci.* 2011, **2**, 204
- 13 Angelos, N.M. Khashab, Y.W. Yang, A. Trabolsi, H.A. Khatib, J.F. Stoddart and J.I. Zink, *J. Am. Chem. Soc.*, 2009, **131**, 12912.
- 14 Z. Zheng, X. Huang, M. Schenderlein, H. Mohwald, G.K. Xu and D.G. Shchukin, *Nanoscale*, 2015, **7**, 2409.
- 15 Z. Zheng, M. Schenderlein, X. Huang, N.J. Brownbill, F. Blanc and D.G. Shchukin, *ACS Applied Materials & Interfaces*, 2015, **7**, 22756.
- 16 A.M. Javier, P. de Pino, M.F. Bedard, D. Ho, A.G. Skirtach, G.B. Sukhorukov, C. Planck and W.J. Parak, *Langmuir*, 2008, **24**, 12517.
- 17 E.V. Skorb, A.G. Skirtach, D.V. Sviridov, D.G. Shchukin and H. Möhwald, *ACS Nano*, 2009, **3**, 1753.
- 18 X. Tao, J.B. Li and H. Mohwald, *Chemistry – A European J.*, 2004, **10**, 3397.
- 19 E.V. Skorb, D.G. Sviridov, H. Möhwald and D.G. Shchukin, *Chemical Communications*, **40**, 6041.
- 20 D.G. Shchukin, D.A. Gorin and H. Mohwald, *Langmuir*, 2006, **22**, 7400.
- 21 K. Köhler, D.G. Shchukin, H. Mohwald and G.B. Sukhorukov, *J. Phys. Chem. B*, 2005, **109**, 18250.
- 22 A.A. Antipov and G.B. Sukhorukov, *Adv. Colloid & Interface Sci.*, 2004, **111**, 49.
- 23 L.P. Lv, S. Jiang, A. Inan, K. Landfester, and D. Crespy, *RSC Advances*, 2017, **7**, 8272.

- 24 D.G. Shchukin, K. Kohler and H. Mohwald, *J. Am. Chem. Soc.*, 2006, **128**, 4560.
- 25 A. Vimalanandan, L.P. Lv, T.H. Tran, K. Landfester, D. Crespy and M. Rohwerder, *Advanced Materials*, 2013, **25**, 6980.
- 26 D.G. Shchukin and H. Möhwald, *ChemComm*, 2011, **47**, 8730.
- 27 D. Borisova, H. Möhwald and D.G. Shchukin, *ACS Nano*, 2011, **5**, 1939.
- 28 I.A. Kartsonakis, I. L. Danilidis, G.S. Pappas and G. Kordas, *Journal of Nanoscience and Technology*, 2010, **10**, 5912.
- 29 J.Tedim, M.L. Zheludkevich, A.N. Salak, A. Lisenkov and M.G.S. Ferreira, *J. Mat. Chemistry*, 2011, **21**, 15464.
- 30 Y.Lvov, W. Wang, L.Q. Zhang and R. Fakhruillin, *Advanced Materials*, 2016, **28**, 1227.
- 31 T.L.P. Galvão, C. S. Neves, A.P.F. Caetano, F. Maia, D. Mata, E. Malheiro, M. J. Ferreira, A. C. Bastos, A.N. Salak, J.R.B. Gomes, J. Tedim and M.G.S. Ferreira, *Journal of Colloid and Interface Science*, 2016, **468**, 86.
- 32 G. Cavallaro, G. Lazzara and R. Fakhruillin, *Therapeutic Delivery*, 2018, **9**, 287.
- 33 S. Bohm, H.N. McMurray, S.M. Powell and D.A. Worsley, *Materials and Corrosion*, 2001, **52**, 896.
- 34 H.N. McMurray, D. Williams, G. Williams and D. Worsley, *Corrosion Engineering Science and Technology*, 2003, **38**, 112.
- 35 A. Ghazi, E. Ghasemi, M. Mahdavian, B. Ramezanzadeh and M. Rostami, *Corrosion Science*, 2015, **94**, 207.
- 36 F. Micciché, H. Fischer, R. Varley and S. van der Zwaag, *Surface & Coating Technology*, 2008, **202**, 3346.
- 37 G.R. Williams and D. O'Hare, *J. Mater. Chem.*, 2006, **16**, 3065.
- 38 E. Alibakhshi, E. Ghasemi, M. Mahdavia and B. Ramezanzadeh, *Corrosion Science*, 2017, **115**, 159.
- 39 G. Williams and H.N. McMurray, *Electrochem. Solid-State Lett.*, 2004, **7**, 13.
- 40 M.H. Kendig and M. Hon, *Electrochem. Solid-State Lett.*, 2005, **8**, 10.
- 41 M.L. Zheludkevich, S.K. Poznyak, L.M. Rodrigues, D. Raps, T. Hack, L.F. Dick, T. Nunes and M.G.S. Ferreira, *Corr. Sci.*, 2010, **52**, 602.
- 42 S.K. Poznyak, J. Tedim, L.M. Rodrigues, A.N. Salak, M.L. Zheludkevich, L.F.P. Dick and M.G.S. Ferreira, *ACS Applied Materials & Interfaces*, 2009, **1**, 2353.
- 43 M.F. Montemor, D.V. Snihirova, M.G. Taryba, S.V. Lamaka, I.A. Kartsonakis, A.C. Balaskas, G.C. Kordas, J. Tedim, A. Kuznetsova, M.L. Zheludkevich and M.G.S. Ferreira, *Electrochimica Acta*, 2012, **60**, 31.
- 44 Tedim, S. K. Poznyak, A. Kuznetsova, D. Raps, T. Hack, M. L. Zheludkevich and M. G. S. Ferreira, *ACS Applied Materials & Interfaces*, 2010, **2**, 1528.
- 45 R.B. Leggat, S.A. Taylor and S.R. Taylor, *Colloids Surf. A*, 2002, **210**, 83.
- 46 J. Chen, Y. Song, D. Shan and E.-H. Han, *Corrosion Science*, 2013, **74**, 130.
- 47 R.-C. Zeng, Z.-G. Liu, F. Zhang, S.Q. Li, H.-Z. Cui and E.-H. Han, *J. Mater. Chem. A*, 2014, **2**, 13049.
- 48 Y.M. Lvov, D.G. Shchukin, H. Möhwald and R.R. Price, *ACS Nano*, 2008, **2**, 814.
- 49 Y. Lvov, W. Wang, L. Zhang, and R. Fakhruillin, *Adv. Mater.*, 2016, **28**, 1227.
- 50 E. Joussein, S. Pitit, J. Churchman, B. Theng, D. Righi and B. Delvaux, *Clay Miner.*, 2005, **40**, 383.
- 51 R. Price, B. Gaber and Y. Lvov, *Journal of Microencapsulation*, 2001, **18**, 713.
- 52 E. Abdullayev, A. Joshi, W.B. Wei, Y.F. Zhao, Yafei and Y. Lvov, *ACS Nano*, 2012, **6**, 7216.
- 53 Y. Lvov and R. Price, *Bio-Inorganic Hybrid Nanomaterials*, E. Ruiz-Hitzky, K. Ariga and Y. Lvov, Eds.; Wiley: London, Berlin, 2007; Chapter 12, pp.419 - 441.
- 54 Y. M. Lvov, D. G. Shchukin, H. Mohwald and R. R. Price, *ACS Nano*, 2008, **2**, 814.
- 55 D. Fix, D.V. Andreeva, Y.M. Lvov, D.G. Shchukin and H. Mohwald, *Adv. Functional. Mater.*, 2009, **19**, 1720.
- 56 E. Abdullayev, R. Price, D. Shchukin and Y.Lvov, *Applied Materials & Interfaces*, 2009, **1**, 1437.
- 57 E. Abdullayev, V. Abbasov, A. Tursunbayeva, V. Portnov, H. Ibrahimov, G. Mukhtarova and Y. Lvov, *Applied Materials & Interfaces*, 2013, **5**, 4464.
- 58 X. Liu, D. Zhang, P. Hou, J. Pan, X. Zhao and B. Hou, *Journal of The Electrochemical Society*, 2018, **165**, 907.
- 59 X. Y. Li, D. Y. Zhang, X. Q. Liu, L. Y. Shi and L. B. Sun, *Chem. Eng. Sci.*, 2016, **141**, 184.
- 60 H. Yin and J. Zhu, *Chem. Eng. J.*, 2016, **285**, 112.
- 61 E. Shchukina, D.G. Shchukin and D.Grigoriev, *Progress in Organic Coatings*, 2018, **123**, 384.
- 62 E. Shchukina, D. Grigoriev, T. Sviridova and D.G. Shchukin, *Progress in Organic Coatings*, 2017, **108**, 84.
- 63 D. Grigoriev, E. Shchukina and D.G.Shchukin, *Advanced Materials Interfaces*, 2017, **4**, 1600318.
- 64 I.A. Kartsonakis and G. Kordas, *J. Am. Ceram. Soc.*, 2010, **93**, 65.
- 65 I.A. Kartsonakis, A.C. Balaskas, E.P. Koumoulos, C.A. Charitidis and G. Kordas, *Corrosion Science*, 2012, **65**, 481.
- 66 M.J. Hollamby, D. Borisova, H. Möhwald and D.G. Shchukin, *Chem. Comm.*, 2012, **48**, 115.
- 67 X. Liu, C. Gu, Z. Wen and B. Hou, *Progress in Organic Coatings*, 2018, **115**, 195.
- 68 N. Y. Abu-Thabit and A.S. Hamdy, *Surface Science and Coatings Technology*, 2016, **303(B)**, 406.
- 69 D.A. Leal, I.C. Riegel-Vidotti, M.G.C. Ferreira and C.E.B. Marino, *Corrosion Science*, 2018, **130**, 56.
- 70 B. Qian, M. Michailidis, M. Bilton, T. Hobson, Z. Zheng and D. Shchukin, *Electrochimica Acta*, in press, DOI: 10.1016/j.electacta.2018.12.062.
- 71 Y. Huang, L. Deng, P. Ju, L. Huang, H. Qian, D. Zhang, X. Li and H.A. Terry, *Mol, ACS Appl. Mater. Interfaces*, 2018, **10**, 23369.
- 72 S. Aryal, C.-M.J. Hu, and L. Zhang, *Small*, 2010, **6**, 1442.
- 73 L. P. Lv, K. Landfester and Daniel Crespy, *Chem. Mater.*, 2014, **26**, 3351.
- 74 Y. Zhao, R. Berger, K. Landfester and Daniel Crespy, *Small*, 2015, **11**, 2995.